

Lecture 1 Fractal Curves and Shapes

1 LENGTH OF COASTLINE

How long is the coast of Britain? The answer to this question can be controversial and depends on the method of measurement. If we were to lay yardsticks of length ϵ along the coastline, the measured result $L(\epsilon)$ equals to the number of yardsticks used $N(\epsilon)$ times ϵ , $L = N\epsilon$. As ϵ becomes smaller, $L(\epsilon)$ gets bigger, and $\lim_{\epsilon \rightarrow 0} L(\epsilon) = \infty$. Empirically, it was found that¹ $L(\epsilon)$ v.s. ϵ follows a power law

$$L(\epsilon) \sim \epsilon^{1-D}. \quad (1)$$

For example, $D = 1.25$ for the west coast of Britain and $D = 1.14$ for the Spain-Portugal border. The exponent D is later to be explained as *fractal dimension* or *Hausdorff-Besicovitch dimension*. Coastlines are generally curves whose Hausdorff-Besicovitch dimension D is a fractional number. These geometric shapes are thus called *fractals*.

In contrast, the length of regular curves, such as straight lines or other smooth curves, are well defined – it does not change with the size of the measuring yardstick. These curves are “rectifiable” and their Hausdorff-Besicovitch dimension is an integer, $D = 1$.

2 DIMENSION AND FRACTAL

The *topological dimension* D_T of geometric shapes in Euclidean space is the number of orthogonal directions or coordinates needed to specify them, which is always an integer. For instance, $D_T = 0$ for a point, $D_T = 1$ for a line or a curve, $D_T = 2$ for a plane or a surface, and $D_T = 3$ for a polyhedron.

Note that, for the above fractal coastline curves, D_T still equals to 1. This gives another definition of fractals:

A *fractal* is a geometric shape (or a set) for which $D > D_T$.

For regular Euclidean shapes, such as points, lines, circles, etc., $D = D_T$.

3 KOCH CURVE

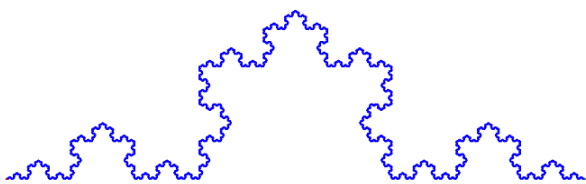


Figure 1: The triadic Koch curve.

The length of the triadic Koch curve $L(\epsilon)$ measured by different ϵ is

$$\begin{aligned} L(1) &= 1 \\ L\left(\frac{1}{3}\right) &= \frac{4}{3} \\ L\left(\frac{1}{9}\right) &= \frac{16}{9} \\ &\dots \end{aligned}$$

In summary,

$$L\left(\frac{\epsilon}{3}\right) = \frac{4}{3}L(\epsilon).$$

Let $L(\epsilon) = C\epsilon^{1-D}$, then $L\left(\frac{\epsilon}{3}\right) = C(\epsilon/3)^{1-D} = (1/3)^{1-D}C\epsilon^{1-D} = (1/3)^{1-D}L(\epsilon)$. So, $(1/3)^{1-D} = 4/3$, namely, $(1/3)^{-D} = 4$. We thus find that

$$D = \log 4 / \log 3 = 1.262$$

for the triadic Koch curve (whose $D_T = 1$).

4 SELF-SIMILARITY

Most fractals are *self-similar*, in the sense that each piece of the shape is geometrically similar to the whole². In particular, if the whole graph is evenly divided into N parts, then each part is similar to (has the same shape of) the original whole graph, but are of smaller size. The ratio of each part to the whole is called the *similarity of ratio* r (< 1). Each part needs to be magnified by $1/r$ times to reproduce the whole. The fractal dimension is then

$$D = \log N / \log(1/r) = -\log N / \log r. \quad (2)$$

In another word,

$$r = 1 / \sqrt[3]{N}. \quad (3)$$

For the triadic Koch curve, $N = 4$ and $r = 1/3$. For a square ($D = D_T = 2$), if $N = 100$, $r = 1/\sqrt{100} = 1/10$.

5 SCALING

Another way to define and extract D is scaling. Consider a metallic ball of uniform density ρ . If the radius R of the ball doubles, then the mass M becomes eight times larger. This results from the fact that $M(R) = \rho \frac{4}{3}\pi R^3$ for this $D = D_T = 3$ geometric object. In this case, we say that the mass of the ball scales with 3rd power of its size R , i.e. $M(R) \sim R^3$. Generally,

$$M(R) \sim R^D \quad (4)$$

allows us to extract the fractal dimension of the object. For the triadic Koch curve, when its size becomes three times bigger ($R \rightarrow 3R$), its mass becomes four times heavier ($M \rightarrow 4M$). That is $M(3R) = C(3R)^D = 3^D CR^D = 3^D M(R) = 4M(R)$, so $3^D = 4$. An equivalent view is to draw a circle (or a sphere) of radius R centered around the object and see how much materials is contained in it.

¹ Mandelbrot, Benoit. "How long is the coast of Britain? Statistical self-similarity and fractional dimension." *Science* 156, no. 3775 (1967): 636-638.

² Some fractals are not strictly self-similar, but are still loosely called self-similar.

6 CANTOR SET

Cantor set or cantor dust, $D_T = 0$ and $D = \log 2 / \log 3 = 0.631$



Figure 2: The first 7 generations of Cantor set.

7 SIERPIŃSKI GASKET

Sierpiński triangle, $D = \log 3 / \log 2 = 1.585$

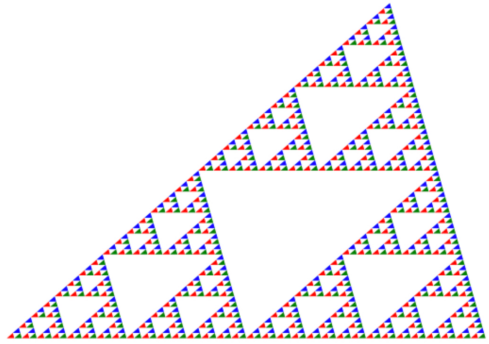


Figure 3: Sierpiński Gasket.

The square version is called Sierpiński carpet, of dimension $D = \log 8 / \log 3 = 1.8928$.

One can also create high dimensional analog with tetrahedrons or cubes (Menger sponge).

8 SPACE-FILLING CURVE

Hilbert curve $D_T = 1$ and $D = 2$.

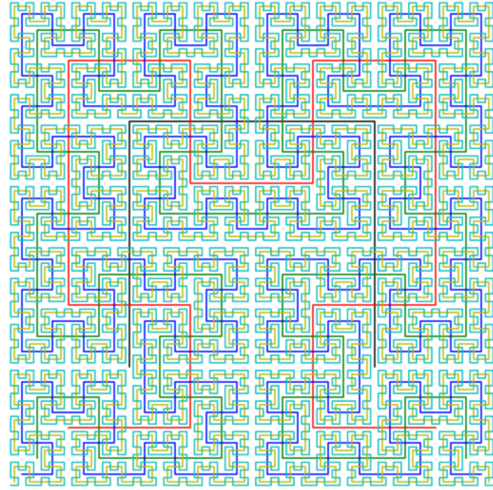


Figure 4: The first 6 generations of Hilbert curve.

Another example of space-filling curve is the Peano curve.

Lecture 2 Fractal Growths

1 TREE

A perfect (binary) tree fractal is characterized by two parameters, the scaling ratio r and the branching angle θ , with the fractal dimension $D = -\log 2 / \log r$ (Figure 1).

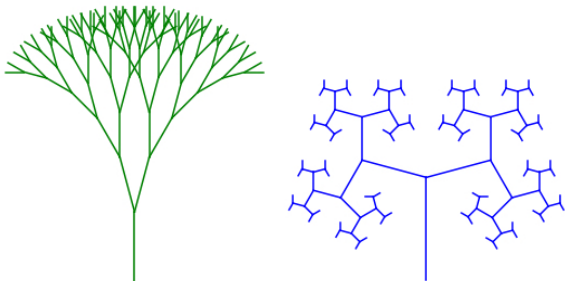


Figure 1: Two trees with $r = 0.8, \theta = 30^\circ$ (left) and $r = 0.65, \theta = 150^\circ$ (right).

or

$$\phi = \frac{1}{\phi - 1}. \quad (3)$$

A *golden rectangle* has a length $a + b$ and a width a such that $\frac{a+b}{a} = \frac{a}{b} = \phi$ (Figure 3).

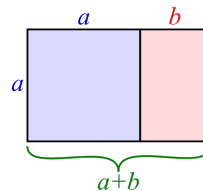


Figure 3: Golden rectangle (Wikipedia).

The Golden ratio also equals to the self-similar fraction expression

$$\phi^* = \frac{1}{1 + \frac{1}{1 + \frac{1}{1 + \frac{1}{1 + \dots}}}}. \quad (4)$$

2.3 Equiangular spiral

An *equiangular spiral* or *logarithmic spiral* (Figure 4) obeys the polar equation

$$r(\theta) = r_0 e^{k\theta} \quad (5)$$

where r is the radius or distance away from the origin and θ is the polar angle that radius vector makes with one axis (here we allow θ to increase beyond 2π).

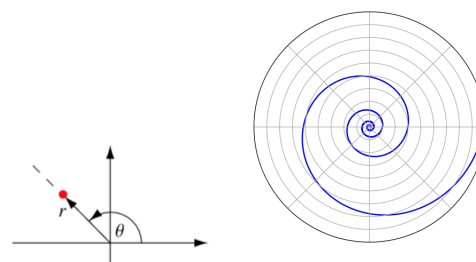


Figure 4: Polar coordinates and the equiangular spiral (Wikipedia).

The parameter r_0 is the initial radius at $\theta = 0$ and the growth factor k defines the angle α that the radius vector makes with the spiral.

$$\frac{dr}{d\theta} = rk \Rightarrow \tan \alpha = \frac{rd\theta}{dr} = k^{-1} \text{ or } k = \cot \alpha$$

Equiangular spirals has interesting properties

- A equiangular spiral cuts each radius vector at a constant angle α (Figure 5).
- A equiangular spiral is self-similar, i.e. its shape is everywhere the same when magnified.
- If a straight line (radius vector) revolves uniformly about its one end point (O) and a point (P) moves along the radius vector with a velocity increasing as its distance from O, then the path described is an equiangular spiral.

$$0, 1, 1, 2, 3, 5, 8, 13, 21, 34, 55, 89, 144 \dots$$

Fibonacci spiral connects quarter-circle arcs inscribed in squares derived from the Fibonacci sequence (Figure 2).

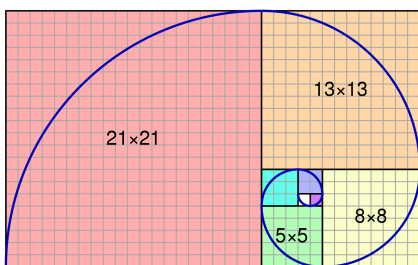


Figure 2: Fibonacci spiral (Wikipedia).

2.2 Golden ratio

The *golden ratio* or *golden mean*

$$\phi = \lim_{n \rightarrow \infty} \frac{F_{n+1}}{F_n} = \frac{1 + \sqrt{5}}{2} \approx 1.618034 \quad (1)$$

$$\text{e.g. } \frac{144}{89} \approx 1.617977528.$$

An alternative definition is to use $\phi^* = \frac{1}{\phi} = \frac{\sqrt{5} - 1}{2} \approx 0.618034$, which is the fraction on a line segment of length 1 such that

$$\frac{1}{\phi^*} = \frac{\phi^*}{1 - \phi^*}, \quad (2)$$

- The radius vector will increase in length in geometrical progression, as it sweeps through successive equal angles.



Figure 5: The logarithmic spiral draw from equally spaced rays, which make equal angles with the spiral. (Wolfram).

The *golden spiral* is an equiangular spiral whose growth factor $k = \frac{\ln \phi}{\frac{\pi}{2}}$ such that the value of r/r_0 is the golden ratio ϕ at the right angle $\theta = \frac{\pi}{2}$. The golden spiral can be approximated by the Fibonacci spiral or similarly, by drawing quarter-circles through successive golden rectangles.

golden spiral \approx Fibonacci spiral

2.4 Golden angle

Golden angle or *Fibonacci angle*

$$\delta = 2\pi(2 - \phi) = \frac{2\pi}{\phi^2} = 2\pi(\phi^*)^2 \approx 2\pi \times 0.381966 \approx 137.51^\circ \quad (6)$$

$$(2 - \phi = 1 + 1 - \phi = 1 - \frac{1}{\phi} = \frac{\phi - 1}{\phi} = \frac{1}{\phi^2} = 1 - \phi^*)$$

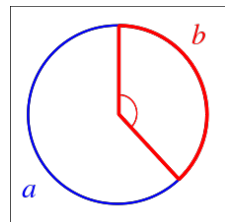


Figure 6: Golden angle is spanned by the smaller arc b when a and b make the golden ratio ϕ . (Wikipedia).

It is also true that

$$\delta = 2\pi \lim_{n \rightarrow \infty} \frac{F_n}{F_{n+2}} \quad (7)$$

e.g. $\frac{55}{144} \approx 0.381944$.

3 FRACTAL AND GOLDEN RATIO

The length ratio of successive branches in trees can be the golden ratio $r = 1/\phi$.¹

Logarithmic spirals are found in the patterns of the Mandelbrot set (Figure 7).

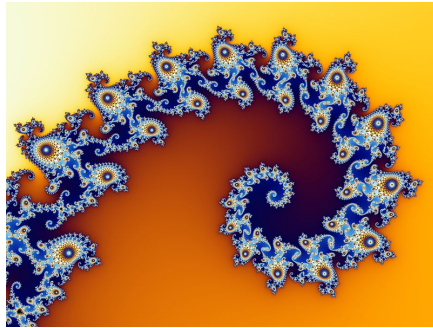


Figure 7: A section of the Mandelbrot set following a logarithmic spiral (Wikipedia).

The tree-like growth of cauliflower is not only fractal, but also featured with spirals (Figure 8).²



Figure 8: Romanesco cauliflower or broccoli (Wikipedia).

Phyllotactic patterns of florets and seeds often have successive pieces making an angle of the golden angle during growth (Figure 9) and globally, exhibit Fibonacci (or approximately golden) spirals.

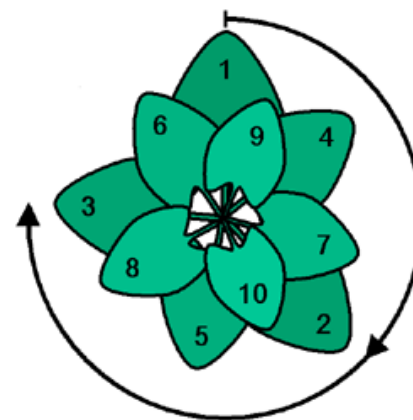


Figure 9: Angle made by successive leaves during growth is the golden angle (Wikipedia).

4 BARNESLEY FERN

Barnsley proposed an iterated function systems (IFS) to generate fern-like leafs by iterative affine transformation of points on a plane (Figure 10).³

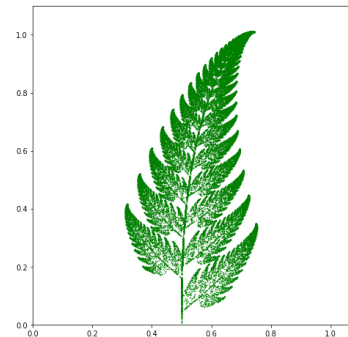


Figure 10: Barnsley fern.

¹Persaud-Sharma, Dharam, and James P. O'Leary. "Fibonacci series, golden proportions, and the human biology." Austin J Surg 2, no. 5 (2015): 1-7.

²Grey, Francois, and Jørgen K. Kjems. "Aggregates, broccoli and cauliflower." Physica D: Nonlinear Phenomena 38, no. 1-3 (1989): 154-159.

³Barnsley, Michael F. Fractals Everywhere. Academic press, 2014.

For a given point $\begin{bmatrix} x \\ y \end{bmatrix}$, one applies rotation and shift to update the point to

$$\begin{bmatrix} x' \\ y' \end{bmatrix} = \begin{bmatrix} a & b \\ c & d \end{bmatrix} \begin{bmatrix} x \\ y \end{bmatrix} + \begin{bmatrix} e \\ f \end{bmatrix}.$$

The rotation matrix $\begin{bmatrix} a & b \\ c & d \end{bmatrix}$ and the shift vector $\begin{bmatrix} e \\ f \end{bmatrix}$ are randomly chosen from one of the four possibilities with probabilities, e.g. 0.85, 0.07, 0.07, 0.01, to draw a point on the smaller level of leafs, left lobe, right lobe, and stem correspondingly.

5 LUNGS AND BLOOD VESSELS

Many tissue structures in human physiology is tree-like and fractal (with randomness) such as lung trachea and blood vessels.⁴

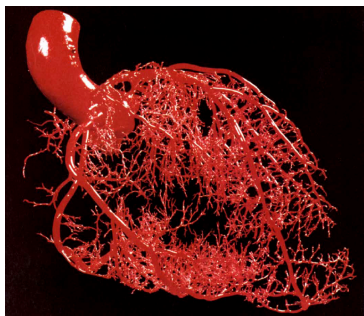


Figure 11: Blood vessels of the heart (Goldberger 1990).

These hierarchical structures are the most efficient way for air / nutrition to reach every cell in the body.

Similarly, river systems and canyons they cut also exhibit fractal structures.

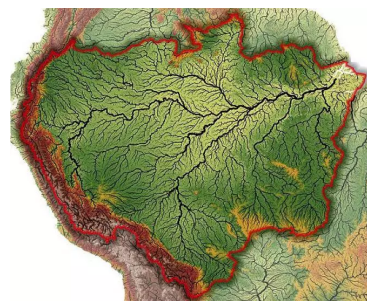


Figure 12: River systems in the Amazon basin (Wikipedia).

6 DIFFUSION-LIMITED AGGREGATION (DLA)

Another way to grow tree-like structures in nature is through the stochastic mechanism of *diffusion-limited aggregation* (DLA).⁵ Patterns like colloidal aggregates and electrical discharge can be explained with it.⁶



Figure 13: Cluster grown from a copper sulfate and high-voltage dielectric breakdown (Wikipedia).

⁴Goldberger, Ary L., David R. Rigney, and Bruce J. West. "Chaos and fractals in human physiology." *Scientific American* 262, no. 2 (1990): 42-49.

⁵Witten Jr, T. A., and Leonard M. Sander. "Diffusion-limited aggregation, a kinetic critical phenomenon." *Physical Review Letters* 47, no. 19 (1981): 1400.

⁶Sander, Leonard M. "Fractal growth processes." *Nature* 322, no. 6082 (1986): 789; Sander, Leonard M. "Fractal growth." *Scientific American* 256, no. 1 (1987): 94-101

Lecture 3 Fractal Mapping

The boundaries of the largest bounded sets are invariant under a complex mapping, e.g. squaring.

1 JULIA SET

Consider the complex mapping

$$z_{n+1} = z_n^2 + c \quad (1)$$

the *Julia set* consists of all initial points z_0 such that $|z_n| < R$ as $n \rightarrow \infty$ (bounded), where R is the escape radius. In practice, one may set, for example, $R = 3.0$ and $n \rightarrow 350$.

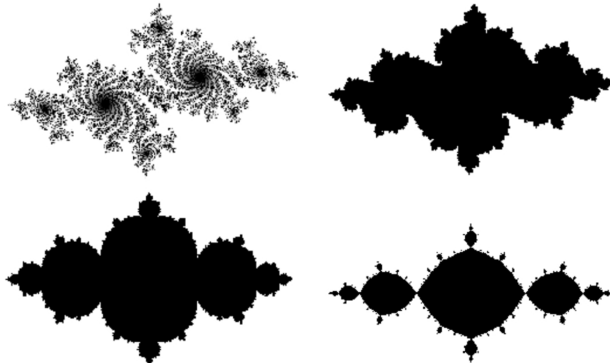


Figure 1: Julia sets for $c = -0.7 + i0.27, -0.7 + i0.1, -0.7, -1$ on the z_0 -complex plane.

3 BURNING SHIP

The burning ship pattern (Figure 3) is contained in the Mandelbrot set of the mapping

$$z_{n+1} = (|\operatorname{Re} z_n| + i|\operatorname{Im} z_n|)^2 + c, z_0 = 0. \quad (3)$$

That is

$$x_{n+1} = x_n^2 - y_n^2 + c_x \quad (4)$$

$$y_{n+1} = 2|x_n y_n| + c_y \quad (5)$$



Figure 3: The burning ship fractal.

2 MANDELBROT SET

Consider the complex mapping

$$z_{n+1} = z_n^2 + c, z_0 = 0, \quad (2)$$

the *Mandelbrot set* consists of all c 's such that $|z_n| < R$ as $n \rightarrow \infty$, where R is the escape radius. In practice, one may set, for example, $R = 3.0$ and $n \rightarrow 350$.

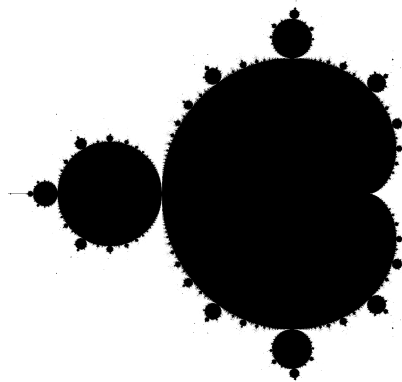


Figure 2: The Mandelbrot set on the c -complex plane.

4 APOLLONIAN PACKING AND SELF-INVERSION

The smallest sets are invariant under geometric inversion.

Three pairwise externally tangent disks S_1, S_2, S_3 are added inside a large disk S_0 and all internally tangent to S_0 . The four circles S_0, S_1, S_2, S_3 are called *initial circles*. Then in each of following steps ($i = 4, 5, \dots$), a disk S_i of maximal possible size is added in S_0 , disjoint from S_1, S_2, \dots, S_{i-1} . The resulted embedded circles are called *Apollonian packing*¹.

For 2d Apollonian disk packing, $D = 1.30568$

For 3d Apollonian sphere packing, $D = 2.4739465^2$

Apollonian packing can also be understood and generated from inversion (Figure 5).

Given a circle C of origin O and radius r , *inversion* with respect to C transforms a point P to Q such that P and Q lie on the same half line from O , and the lengths satisfy (Figure 4)

$$|OP||OQ| = r^2.$$

¹Sometimes, the name Apollonian packing is reserved exclusively for the case that S_1, S_2, S_3 are of equal size.

²Borkovec, Micha, Walter De Paris, and Ronald Peikert. "The fractal dimension of the Apollonian sphere packing." *Fractals* 2, no. 04 (1994): 521-526.

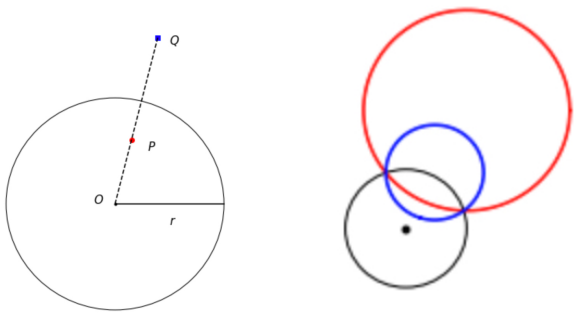


Figure 4: Left: inversion of a point P to Q . Right: inversion of a circle (blue) to a circle (red), vice versa.

- circles passing through O invert into straight lines not passing through O , vice versa
- circles orthogonal to C and straight lines passing through O are invariant under inversion
- generally, circles not passing through O invert into circles

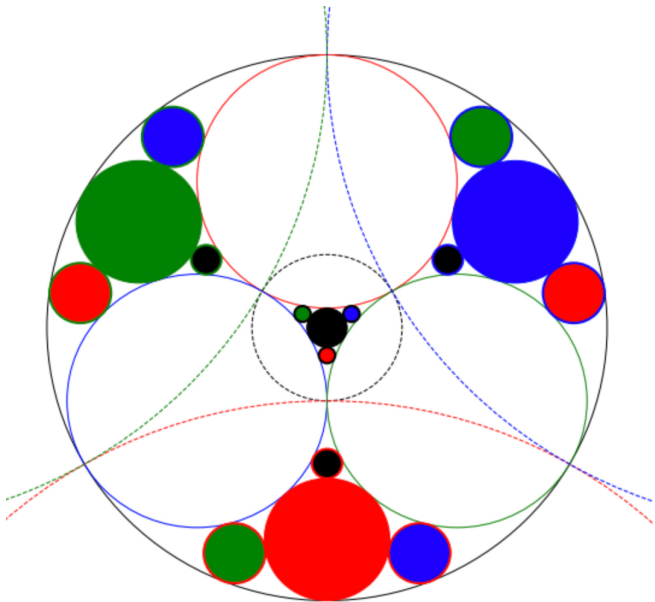


Figure 5: Apollonian disk packing. Initial circles S_0 (big black solid), S_1 (big red solid), S_2 (big blue solid), S_3 (big green solid). Inversion circles C_0 (black dashed), C_1 (red dashed), C_2 (blue dashed), C_3 (green dashed). In the first generation, S_4 is from inversion of S_0 with respect to C_0 , denoted by $S_4 = S_0 : C_0$ (black filled). Similarly, $S_5 = S_1 : C_1$ (red filled), $S_6 = S_2 : C_2$ (blue filled), $S_7 = S_3 : C_3$ (green filled). The second generation contains 12 members, which are inversion of S_4, S_5, S_6, S_7 with respect to three out of the four C_0, C_1, C_2, C_3 .

Lecture 4 Fractal Scaling

1 FRACTALS ARE SCALE-FREE

Fractals are self-similar in a sense that a small portion has the same shape as the whole, and if appropriately magnified, can reproduce the entire pattern. They are *scale invariant* – patterns do not change after a scaling transformation. This indicates that fractals are *scale-free*, i.e. there is no typical characteristic (length) scale for a fractal and there are detailed structures on all scales. One cannot easily tell the difference between two pictures of a fractal at different magnification ratios, if no other information is provided. Scale-free system often contains some type of fractal pattern (with randomness) within it.

For example, it is hard to answer the question “what is the typical length of branches in a tree?”. From the largest trunk (~ 10 m) to the smallest leaf stripes (~ 1 cm), the length spans four orders of magnitude. A mathematical fractal has structures spanning infinitely many orders of magnitude.

In contrast, many systems in nature do possess a characteristic scale. For example, the typical height L_0 of a person is on the order of ~ 1 m. The variation of individual heights in the population is around this typical L_0 and may be described by a bell-shaped distribution curve peaked around, say $L_0 = 1.7$ m.

2 POWER-LAW DISTRIBUTION

Scale-free systems like fractals follow the power-law distribution (Zipf's law)¹. A continuous power-law distribution with exponent $\alpha > 0$

$$p(x) = Cx^{-\alpha} = C \frac{1}{x^\alpha}, \quad x > x_{\min}, \quad (1)$$

or the discrete version

$$p(k) = Ck^{-\alpha}, \quad k = k_1, k_2, k_3, \dots. \quad (2)$$

On the log-log plot, a power-law distribution appears to be a line with a slope equal to the exponent α (Figure 1).

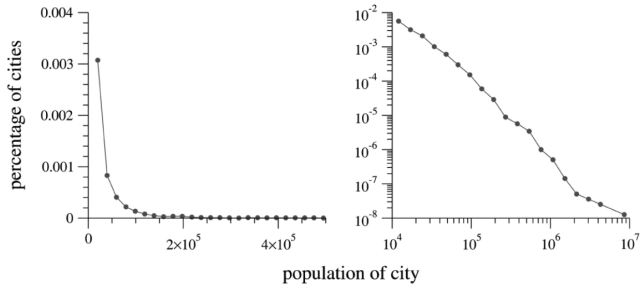


Figure 1: Population size of US cities (2000) on the linear plot and the log-log plot. (Newman, 2005)

Power-law distributions have long tails that span over many orders of magnitude.

Examples of power-law distributed systems (approximately over certain orders of magnitude) are

- size of craters on the Moon
- frequency of words in human language
- population size of cities
- magnitude of earthquake (Gutenberg-Richter law)
- stream number H_w of rivers of order w (Horton's law²)
- number of links of webpages
- spatial distribution of stars and galaxies in the universe
- domain sizes at the critical point of the second order phase transition (this is an equilibrium system)
- size of extinction events
- occurrence of forest fires
- $1/f$ noise of quasar intensity (power spectrum)

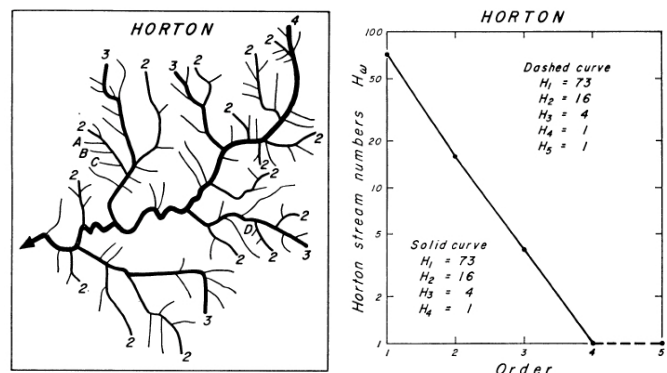


Figure 2: Stream number H_w of rivers of order w under Horton's law (Shreve, 1966). Smaller branches have smaller orders.

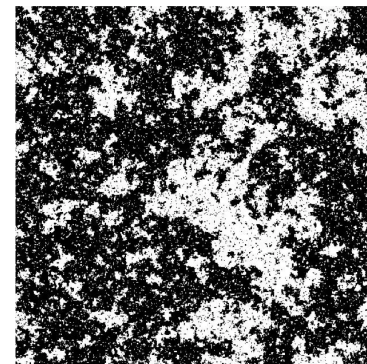


Figure 3: Magnetic moment or liquid droplets (black pixels) at the critical point of 2nd order phase transitions.

¹Newman, M. E. J. "Power laws, Pareto distributions and Zipf's Law. In: B. McKelvey (Ed.). 2013." Complexity. Critical Concepts 5 (2013): 15-67.

²Shreve, Ronald L. "Statistical law of stream numbers." The Journal of Geology 74.1 (1966): 17-37.

3 BROWNIAN MOTION AND STOCK MARKET

Temporal properties such as stock prices (modeled by Brownian motion) can also exhibit scale-free fractal patterns (Figure 4). When seen at different time scales, e.g. over days, weeks, months or years, the noisy profile of stock prices or Brownian motion is similar to each other.

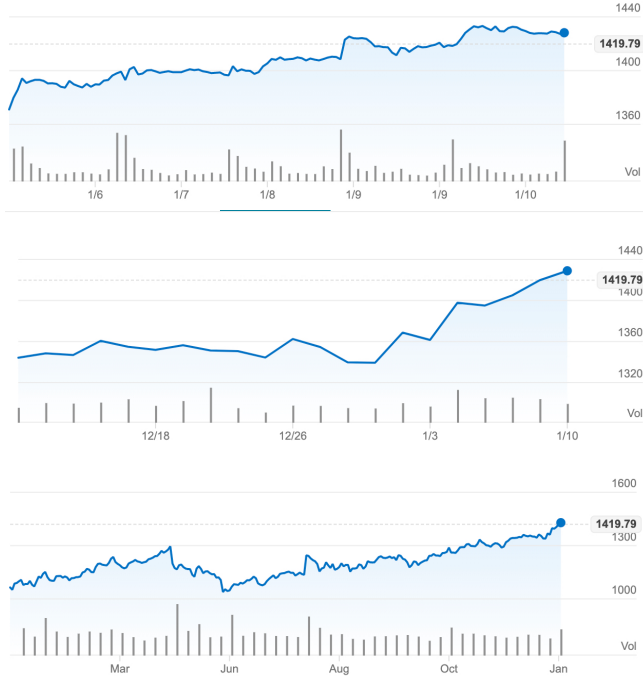


Figure 4: Stock price of Google over one week, one month and one year (2019-2020).

4 SCALE-FREE NETWORKS

Networks consist of points (*nodes*) connected by links (*edges*), for example,

- computer network
- internet or world wide web
- social network
- protein interaction network³
- ecological network
- airport traffic network

The number of edges connected to a node is called its *degree*. Some (not all) networks are scale-free, i.e. the number of nodes with a certain degree follows a power-law distribution⁴.

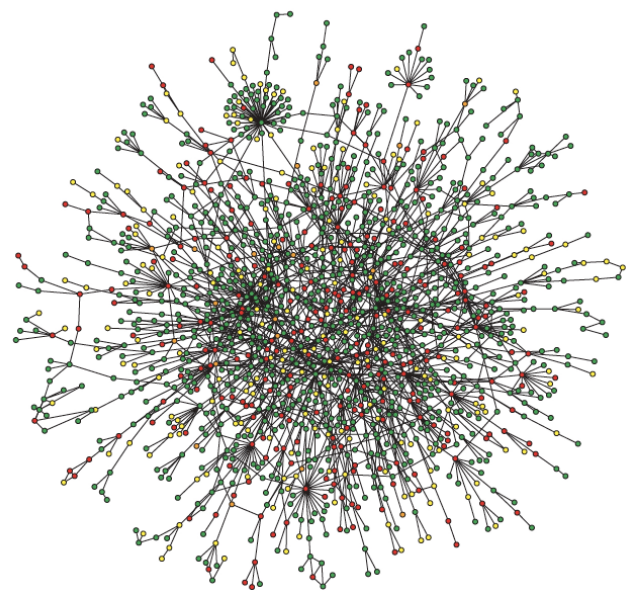


Figure 5: Yeast protein interaction network. (Barabasi 2004)

5 SELF-ORGANIZED CRITICALITY AND EARTHQUAKE

Earthquakes or avalanches, or broadly speaking, the phenomenon of self-organized criticality (SOC) can be explained by the sandpile model. The magnitude of earthquakes or avalanches follows a power law (Gutenberg-Richter relationship)⁵.

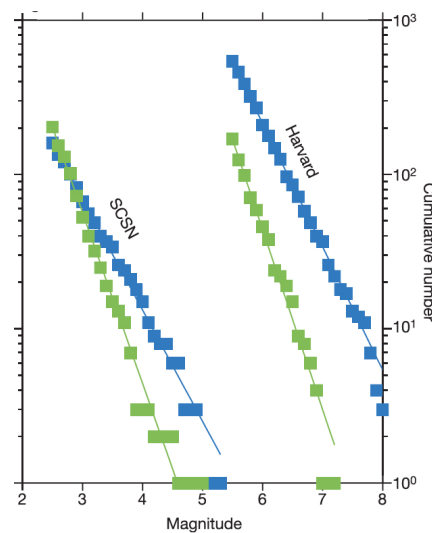


Figure 6: The distribution of earthquake magnitude. (Schorlemmer, 2005)⁶

The **sandpile model** was proposed by Per Bak, Chao Tang and Kurt Wiesenfeld to explain the universal occurrence of self-organized criticality (SOC)⁷. On a discrete lattice, for example a two-dimensional $L \times L = 100 \times 100$ grid, the number of grains, $Z_n(x,y)$ at site (x,y) and time moment n can be 0, 1, 2, 3, 4. One randomly drop a new grain at a site, which increases Z_n by one,

³Barabási, A., Oltvai, Z. Network biology: understanding the cell's functional organization. *Nat Rev Genet* 5, 101–113 (2004) doi:10.1038/nrg1272

⁴Barabási, Albert-László, and Réka Albert. "Emergence of scaling in random networks." *Science* 286, no. 5439 (1999): 509-512.

⁵Wesnousky, Steven G. "The Gutenberg-Richter or characteristic earthquake distribution, which is it?." *Bulletin of the Seismological Society of America* 84, no. 6 (1994): 1940-1959.

⁶Schorlemmer, Danijel, Stefan Wiemer, and Max Wyss. "Variations in earthquake-size distribution across different stress regimes." *Nature* 437, no. 7058 (2005): 539.

⁷Bak, Per, Chao Tang, and Kurt Wiesenfeld. "Self-organized criticality." *Physical Review A* 38.1 (1988): 364.

i.e.

$$Z_{n+1}(x, y) = Z_n(x, y) + 1.$$

If Z_n of a certain site reaches a threshold value, say $Z_c = 4$, a toppling event is triggered which spreads all the grains at that site to its neighboring sites, i.e.

$$Z_n(x, y) = 0$$

$$Z_n(x \pm 1, y) = Z_n(x \pm 1, y) + 1$$

$$Z_n(x, y \pm 1) = Z_n(x, y \pm 1) + 1$$

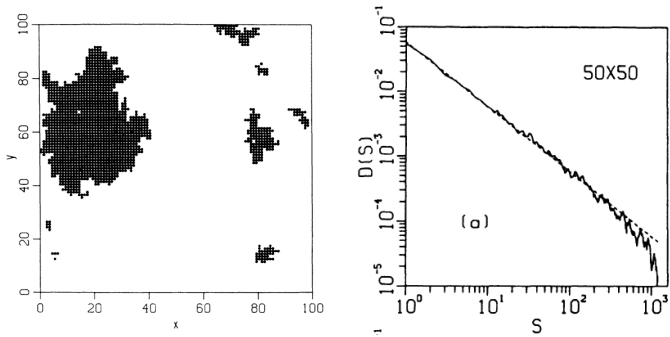


Figure 7: An avalanche in the 50×50 sandpile model. The distribution of avalanche sizes. (Bak, 1988)

A collective toppling event involving many grains is an **avalanche**. The number of sites involved in an avalanche is its size. The distribution of the sizes of avalanches follows the Gutenberg-Richter relationship.